

3 EFFECT OF STRESS RATIO ON FATIGUE-CRACK GROWTH  
IN 7075-T6 ALUMINUM-ALLOY SHEET 6

By C. Michael Hudson and Joseph T. Scardina

1 NASA Langley Research Center  
Langley Station, Hampton, Va. 3

Presented at the National Symposium on Fracture Mechanics

GPO PRICE \$ \_\_\_\_\_

CFSTI PRICE(S) \$ \_\_\_\_\_

Hard copy (HC) 3.00

Microfiche (MF) .65

ff 653 July 65

Bethlehem, Pennsylvania  
June 19-21, 1967

FACILITY FORM 502

**N 68-27473**

(ACCESSION NUMBER)

24  
(PAGES)

TMX-60125  
(NASA CR OR TMX OR AD NUMBER)

(THRU)

1  
(CODE)

17  
(CATEGORY)

# EFFECT OF STRESS RATIO ON FATIGUE-CRACK GROWTH

## IN 7075-T6 ALUMINUM-ALLOY SHEET

By C. Michael Hudson and Joseph T. Scardina

### ABSTRACT

Axial-load fatigue-crack-propagation tests were conducted on 12-inch- (305-mm) wide sheet specimens made of 7075-T6 aluminum alloy. These tests were made at stress ratios  $R$  (ratio of the minimum stress to the maximum stress) ranging from -1.0 to 0.8 and at maximum stress levels ranging from 5 to 50 ksi (34 to 340 MN/m<sup>2</sup>) to study the effects of stress ratio on fatigue-crack growth. The fatigue-crack-propagation data were analyzed using Paris' stress-intensity analysis. The data from tests at negative  $R$  values fell into a relatively narrow scatterband along with the results from the  $R = 0$  tests on a plot of rate against stress-intensity range. Apparently, the compression portion of the loading cycle did not significantly affect crack growth in these tests. The data from tests at different positive stress ratios fell into discrete bands on these plots. These bands varied systematically with  $R$ , that is, the higher the stress ratio at a given value of  $\Delta K$ , the higher the rate of fatigue-crack growth. This spread in rates was small at the lower stress-intensity range, but became progressively larger as the stress-intensity range was increased.

Semiempirical equations developed by Forman, et al., by Broek and Schijve, and by Paris were fitted to the data from this investigation using a least squares fit. Forman's equation gave the best fit to the data.

The fracture surfaces of the specimens changed from the normal mode to a shear mode within a reasonably narrow range of crack growth rates for all  $R$  values. The stress-intensity range at transition was approximately a constant for tests at negative stress ratios. Forman's equation adequately represented the variation between the stress ratio and the stress-intensity range at positive stress ratios.

EFFECT OF STRESS RATIO ON FATIGUE-CRACK GROWTH  
IN 7075-T6 ALUMINUM-ALLOY SHEET

By C. Michael Hudson\* and Joseph T. Scardina\*\*

NASA Langley Research Center  
Langley Station, Hampton, Va.

INTRODUCTION

Fatigue cracks frequently grow during a large portion of the life of cyclically loaded components. Therefore, any parameter which significantly affects the growth of fatigue cracks can have a major effect on the total fatigue behavior of the components. One such parameter is the stress ratio  $R$  (ratio of the minimum stress to the maximum stress). Accordingly, an investigation has been conducted to determine the effects of a wide range of  $R$  values and stresses on fatigue-crack growth in 7075-T6 aluminum-alloy sheet specimens. This material was selected because of its frequent use in aircraft construction.

The data were analyzed using Paris' stress-intensity method (ref. 1) which is based on fracture mechanics considerations. Figge and Newman (ref. 2) showed that by using this method the data from simple sheet specimens could be used to predict fatigue-crack-growth behavior in simulated structural configurations. Semiempirical equations developed by Forman, et al. (ref. 3), by Broek and Schijve (ref. 4), and by Paris (ref. 1) were fitted to the data generated in this investigation using least squares techniques.

The crack lengths and crack propagation rates at the transition from the normal to the shear mode on the failure surfaces were determined. A study was made to determine whether a relationship existed between the stress ratio and the stress-intensity range at transition.

SYMBOLS

The units used for the physical quantities defined in this paper are given both in U.S. Customary Units and in the International System of Units, SI (ref. 5). The appendix presents factors relating these two systems of units.

- $a$  one-half of the total length of a central symmetrical crack, in. (mm)  
 $a_f$  half-length of crack immediately prior to rapid fracture, in. (mm)

---

\*Materials Engineer.

\*\*Aerospace Engineer.

|                    |                                                                                                                                                       |
|--------------------|-------------------------------------------------------------------------------------------------------------------------------------------------------|
| $a_i$              | half-length of crack at onset of slow crack growth, in. (mm)                                                                                          |
| $a_t$              | half-length of crack at which transition of the failure surface from the normal mode to the shear mode began, in. (mm)                                |
| $C, C_1, C_2, C_3$ | constants in fatigue-crack propagation equations                                                                                                      |
| $K_c$              | critical stress-intensity factor for failure, $\text{psi-in}^{1/2}$ ( $\text{MN/m}^{3/2}$ )                                                           |
| $K_{\max}$         | stress-intensity factor corresponding to maximum cyclic stress, using tangent formula width correction, $\text{psi-in}^{1/2}$ ( $\text{MN/m}^{3/2}$ ) |
| $K'_{\max}$        | stress-intensity factor corresponding to maximum cyclic stress, using Broek's width correction, $\text{psi-in}^{1/2}$ ( $\text{MN/m}^{3/2}$ )         |
| $K_{\min}$         | stress-intensity factor corresponding to minimum cyclic stress, using tangent formula width correction, $\text{psi-in}^{1/2}$ ( $\text{MN/m}^{3/2}$ ) |
| $K'_{\min}$        | stress-intensity factor corresponding to minimum cyclic stress by using Broek's width correction, $\text{psi-in}^{1/2}$ ( $\text{MN/m}^{3/2}$ )       |
| $\Delta K$         | range of the stress-intensity factor (with tangent width correction), $K_{\max} - K_{\min}$ , $\text{psi-in}^{1/2}$ ( $\text{MN/m}^{3/2}$ )           |
| $\Delta K_t$       | range of the stress-intensity factor at transition, $\text{psi-in}^{1/2}$ ( $\text{MN/m}^{3/2}$ )                                                     |
| $\Delta K'$        | range of the stress-intensity factor (with Broek's width correction), $\text{psi-in}^{1/2}$ ( $\text{MN/m}^{3/2}$ )                                   |
| $m, n$             | exponents in fatigue-crack-growth equation                                                                                                            |
| $N$                | number of cycles                                                                                                                                      |
| $P_a$              | alternating load, kips (newtons)                                                                                                                      |
| $P_f$              | load on specimen immediately prior to rapid fracture, kips (newtons)                                                                                  |
| $P_i$              | load on specimen at onset of slow crack growth, kips (newtons)                                                                                        |
| $P_m$              | mean load, kips (newtons)                                                                                                                             |
| $P_{\max}$         | maximum load applied in a cycle, $P_m + P_a$ , kips (newtons)                                                                                         |

|           |                                                                   |
|-----------|-------------------------------------------------------------------|
| $P_{min}$ | minimum load applied in a cycle, $P_m - P_a$ , kips (newtons)     |
| R         | ratio of minimum stress to maximum stress                         |
| $S'_a$    | alternating net stress, $P_a/(w - x)t$ , ksi (MN/m <sup>2</sup> ) |
| $S'_m$    | mean net stress, $P_m/(w - x)t$ , ksi (MN/m <sup>2</sup> )        |
| $S_{max}$ | maximum gross stress, $P_{max}/wt$ , ksi (MN/m <sup>2</sup> )     |
| $S_{min}$ | minimum gross stress, $P_{min}/wt$ , ksi (MN/m <sup>2</sup> )     |
| $S_o$     | maximum net stress, $P_{max}/(w - x)t$ , ksi (MN/m <sup>2</sup> ) |
| t         | specimen thickness, in. (mm)                                      |
| w         | specimen width, in. (mm)                                          |
| x         | length of the crack starter notch, in. (mm)                       |
| $\alpha$  | correction for finite width of panel                              |

## SPECIMENS, TESTS, AND PROCEDURES

### Specimens

The material was taken from the special stock of 7075-T6 aluminum-alloy sheet retained at Langley Research Center for fatigue testing. The fatigue properties of this material are discussed in reference 6. The tensile properties of the sheet are given in table I. The specimen configuration is shown in figure 1. Sheet specimens 12 inches wide (305 mm), 35 inches (891 mm) long, and with a nominal thickness of 0.090 inch (2.28 mm) were tested.

A notch 0.10 inch (2.5 mm) long by 0.01 inch (0.25 mm) wide was cut into the center of each specimen using an electrical discharge process. Very localized heating occurs in making notches in this manner. Thus, virtually all of the material through which the fatigue crack propagates is unaltered by the cutting process. All specimens were made with the longitudinal axis of the specimens parallel to the rolling direction of the sheet.

A reference grid (ref. 7) was photographically printed on the surface of the specimens to mark intervals in the path of the crack. Metallographic examination and tensile tests conducted on specimens bearing the grid indicated that the grid had no detrimental effect on the material.

## Testing Machines

Four axial-load fatigue testing machines were employed in this investigation: a 20,000-lbf- (89-kN) capacity subresonant fatigue machine (ref. 8) having an operating frequency of 1800 cpm (30 Hz); a 100,000-lbf- (445-kN) capacity hydraulic fatigue machine (ref. 9) which applied loads at a rate of 1200 cpm (20 Hz); a 120,000-lbf- (553-kN) capacity jack (ref. 10) having a loading frequency of 30 cpm (0.5 Hz), and a combination hydraulic and subresonant fatigue testing machine (ref. 11) capable of applying loads up to 132,000 pounds (587 kN) hydraulically or 105,000 pounds (466 kN) subresonantly. The operating frequencies were 40 to 60 cpm (0.7 to 1 Hz) for the hydraulic unit, and approximately 820 cpm (14 Hz) for the subresonant unit.

Loads were continuously monitored on these machines by measuring the output of a strain-gage bridge attached to a dynamometer in series with the specimens. The maximum error in loading was  $\pm 1$  percent of the applied load.

## Test Procedure

Axial-load fatigue-crack-propagation tests were conducted at stress ratios ranging from -1.0 to 0.8. Generally, tests were conducted at a number of stress levels (ranging from 5 to 50 ksi (34 to 340 MN/m<sup>2</sup>)) for a given stress ratio. Duplicate tests were conducted at each stress level. The mean and alternating loads were kept constant throughout each test.

Fatigue crack growth was observed through 10-power microscopes while illuminating the specimen with stroboscopic light. The number of cycles required to propagate the crack to each grid line was recorded so that crack-propagation rates could be determined. Approximately two-thirds of the crack-propagation tests were conducted to failure. The remaining one-third were stopped before failure, and the cracked specimens used in residual-static-strength tests.

In all of the tests (crack growth and residual static strength), the specimens were clamped between lubricated guides in order to prevent buckling and out-of-plane vibrations during testing. Light oil was used to lubricate the surfaces of the specimens and the guides. None of this oil was observed to enter the crack during testing. Consequently, the oil was not expected to affect the crack growth. Ethyl alcohol was periodically sprayed on the specimen surface to more clearly indicate the crack front. A cutout 1/8 inch (3.18 mm) wide was made across the width of one guide plate to allow visual observation of the crack-growth region.

Axial-load residual-static-strength tests were conducted at a load rate of 120,000 lbf/min (10 kN/s), using the unfailed crack-propagation specimens. A 70-mm sequence camera operating at 20 frames per second was used to obtain slow crack-growth data. The cracked section of the specimen and the image of a load-indicating device were photographed on each frame of film by using an optical prism. From this film, the load at which the crack first started to grow statically and the load and crack length immediately prior to final failure were determined.

## Method of Analysis

The fatigue-crack-growth data were analyzed by using the stress-intensity method (ref. 1) which is based on fracture mechanics considerations. This method hypothesized that the rate of fatigue-crack propagation was a function of the stress-intensity range, that is

$$\frac{da}{dN} = f(\Delta K) \quad (1)$$

where

$$\Delta K = K_{\max} - K_{\min} \quad (2)$$

For centrally cracked specimens subjected to a uniformly distributed axial load

$$K_{\max} = S_{\max} \sqrt{\alpha a} \quad (3)$$

and

$$K_{\min} = S_{\min} \sqrt{\alpha a} \quad (4)$$

The term  $\alpha$  is a factor which corrects for the finite width of the specimen and is given by:

$$\alpha = \sqrt{\frac{w}{\pi a} \tan \frac{\pi a}{w}} \quad (5)$$

The term  $S_{\max}$  is the maximum gross stress in the cycle and  $S_{\min}$  is the minimum gross stress in the cycle. In presenting the results, the experimental values of  $da/dN$  were plotted against  $\Delta K$  (eq. (2)).

## RESULTS AND DISCUSSION

### Fatigue-Crack-Growth Rates

The fatigue-crack-growth curves (plots of half-crack length against number of cycles) from duplicate tests were plotted on a single figure, and an average curve derived. The difference in the number of cycles required to reach a given crack length in duplicate tests seldom exceeded 20 percent. All of the fatigue-crack-growth data presented in the next three sections were obtained from these average curves. The number of cycles required to propagate the cracks from a half-length  $a$  of 0.10 in. (2.54 mm) to specified half-crack lengths is shown in table II. Fatigue-crack-propagation rates,  $da/dN$ , were determined graphically by taking the slopes of the crack-growth curves defined in table II.

## Effect of Stress Ratio

The fatigue-crack-propagation data are presented in plots of rate against the stress-intensity range  $\Delta K$ . The data from tests at all negative  $R$  values fell into a relatively narrow scatterband along with the data from  $R = 0$  tests (see fig. 2) when the compression portion of the loading cycle was neglected in calculating  $\Delta K$ . That is, for  $R < 0$ ,  $\Delta K$  in equation (2) became  $K_{\max}$ . Apparently, the compression portion of the loading cycle did not significantly affect fatigue-crack growth in these tests. This finding is consistent with that of Illg and McEvily (ref. 12) who found no effect of compressive loading on crack propagation in a limited number of tests on 7075-T6.

The data from all tests at a given positive  $R$  value fell into a discrete scatterband on the plots of rate against  $\Delta K$  (fig. 3). These scatterbands varied systematically with  $R$ , that is, the higher the stress ratio, the higher the rate of fatigue-crack growth for a given value of  $\Delta K$ . This spread in rates for different values of  $R$  became larger as  $\Delta K$  increased. In contrast to this finding, all of the data from tests at  $R$  values ranging from 0 to 0.85 fell into the same scatterband for Ti-8Al-1Mo-1V (Duplex Annealed), ref. 13.

## Correlation of Data With Fatigue-Crack Growth

Empirical fatigue-crack-growth equations developed by Forman, et al., (ref. 3), by Broek and Schijve (ref. 4), and by Paris (ref. 1) were fitted to the test data. Forman's and Broek's equations contained  $R$  as an explicit function while Paris' equation did not. Least squares techniques were used to determine the appropriate constants for the various equations. (NOTE: The constants given in this report for these equations are for U.S. Customary Units only!) In fitting these equations, all of the data from  $R < 0$  tests were assumed to apply to  $R = 0$  tests since all of the data for  $R \leq 0$  fell into the same scatterband.

The empirical equation developed by Forman, et al. (ref. 3), relating  $da/dN$ ,  $\Delta K$ ,  $R$ , and  $K_c$  (the critical stress-intensity factor at failure) produced excellent fit to the data (fig. 4). This equation has the form:

$$\frac{da}{dN} = \frac{C(\Delta K)^n}{(1 - R)K_c - \Delta K} \quad (6)$$

where  $C$  and  $n$  are empirically determined constants. The value of  $K_c$  was obtained from the auxiliary residual static strength tests. This factor is related to the load at rapid fracture  $P_f$ , the associated crack length  $a_f$ , and the width-correction factor  $\alpha$  as follows:

$$K_c = \left( P_f / wt \right) \sqrt{a_f} \alpha \quad (7)$$



An average value of  $K_C$  of 40,400 psi-in<sup>1/2</sup> (40.7 MN/m<sup>3/2</sup>) was found in these tests (table III). The constants  $C$  and  $n$  in equation (6) were calculated to have values of  $2.13 \times 10^{-13}$  and 3.21, respectively. These values are close to the values obtained in reference 3 for 7075-T6 aluminum-alloy sheet tested at a limited number of stress ratios.

The equation developed by Broek and Schijve (ref. 4) was also fitted to the test data (fig. 5). This equation has the form:

$$\frac{da}{dN} = C_1 (K'_{\max})^3 \exp(-C_2 R) \quad (8)$$

where

$$K'_{\max} = S_{\max} \sqrt{a} \sqrt[3]{1 + 40(a/w)^2} \quad (9)$$

Equation (8) can also be written in terms of the stress-intensity range as

$$\frac{da}{dN} = C_1 \left( \frac{\Delta K'}{1 - R} \right)^3 \exp(-C_2 R) \quad (10)$$

The constants  $C_1$  and  $C_2$  were determined to be  $6.93 \times 10^{-17}$  and 3.85, respectively. The curves computed by equation (10) are shown in figure 5. Broek's equation does not fit the test data particularly well, especially at the higher crack-growth rates for either positive, zero, or negative  $R$  values. The sums of the squares of the differences between the logarithms of the observed rates and those of the calculated rates were three times larger for Broek's equation than for Forman's. (These are the sums which were minimized by using least squares techniques.)

Paris (ref. 1) proposed the following relationship between the rate of fatigue-crack growth and the stress-intensity range:

$$\frac{da}{dN} = C_3 (\Delta K)^m \quad (11)$$

where  $C_3$  is a constant which is proposed to incorporate the effects of material, mean load, loading frequency, and environment. (The functional form of eq. (11) is shown by eq. (1).) Paris found the broad trend of the data is characterized by equation (11) where  $m = 4$ . This equation produced a reasonably good fit to the data (fig. 6). Separate values of the coefficient  $C_3$  had to be computed for each  $R$  value since  $R$  is not an explicit function in equation (11). These coefficients are listed in the following table:

| R        | $C_3$                  |
|----------|------------------------|
| $\leq 0$ | $5.52 \times 10^{-21}$ |
| .2       | $6.44 \times 10^{-21}$ |
| .33      | $1.00 \times 10^{-20}$ |
| .5       | $1.80 \times 10^{-20}$ |
| .7       | $3.95 \times 10^{-20}$ |
| .8       | $6.84 \times 10^{-20}$ |

Comparison of figures 4 and 6 shows that Forman's equation fits the data from this investigation somewhat better than Paris'. The sum of the squares of the differences between the logarithms of the observed rates and those of the calculated rates was one and one-half times larger for Paris' equation than for Forman's. The superiority of Forman's equation is even further exemplified by the fact that it fit the data better with only two empirical constants than Paris' equation did with six.

The data on each plot in figure 4 fell in a narrow band that has an "S" shape or reflex type of curvature. A reflex curvature is also obtained from Forman's equation, which is induced by  $\Delta K$  approaching  $(1 - R)K_C$  in the denominator of equation (6). This intrinsic shape is the primary reason for the excellent fit obtained using Forman's equation. Broek's and Paris' equations do not provide for this reflex curvature.

#### Fatigue-Crack-Growth Behavior at Transition in Fracture Mode

The fracture surfaces of the broken specimens were inspected to determine the crack lengths at which the transition from the normal mode (fracture surface normal to the sheet surface and loading direction) to a shear mode (fracture surface  $45^\circ$  to the sheet surface) began. The values of  $da/dN$ ,  $\Delta K$ , and  $R$  associated with transition in each test are listed in table IV. (NOTE: The rates at transition listed in table IV were obtained from the crack-growth curves for the individual tests rather than from the average curves in table II.) The transitions began within a reasonably narrow range of crack-growth rates ( $8.8 \times 10^{-6}$  to  $2.9 \times 10^{-5}$  in./cycle (200 to 730 nm/cycle)) for all  $R$  values. Broek and Schijve (ref. 4) similarly found that the rate of crack growth was approximately constant when the transition was completed rather than beginning.

In 45 of the 92 tests conducted, the transition to the shear mode began at the crack starter notch. The value of  $a_t$  in these tests has been designated  $\leq 0.05$  in. (13 mm) in table IV. The fatigue-crack-growth rates measured in these 45 tests were never lower than  $2.9 \times 10^{-5}$  in./cycle (730 nm/cycle),

the apparent upper limit of the range of rates at transition for the remaining tests.

The stress-intensity range at transition  $\Delta K_t$  was approximately a constant for  $R \leq 0$  (fig. 7). At  $R > 0$ , Forman's equation (eq. (6)) gave a good approximation of the relationship between  $\Delta K$  and  $R$  when a crack-growth rate of  $1.40 \times 10^{-5}$  in./cycle (which is within the narrow range of crack-growth rates at transition) was assumed at transition (see fig. 7). The values of  $C$ ,  $n$ , and  $K_c$  were known as discussed previously. Substituting these values into equation (6) gave the following nonlinear relationship between  $\Delta K$  and  $R$  at transition for these tests:

$$R = 1 - \frac{1.52 \times 10^{-8} (\Delta K)^{3.21} + \Delta K}{40400} \quad (12)$$

Contrary to this finding, Wilhem (ref. 14) reported a linear relationship between  $\Delta K$  and  $R$  at transition for aluminum alloys tested at positive  $R$  values.

At transition the fracture surfaces changed from the normal mode to single, double, or dual (single at one end of the crack and double at the other) shear mode (see table IV). No relationship was apparent between the type of shear mode (single, double, or dual) and the applied stress level.

#### CONCLUSIONS

Axial-load fatigue-crack-propagation tests were conducted on sheet specimens 12 in. (305 mm) wide and nominally 0.090 in. (2.28 mm) thick made of 7075-T6 aluminum alloy. These tests were at stress ratios  $R$  ranging from -1.0 to 0.8, and at maximum stresses ranging from 5 to 50 ksi (34 to 340 MN/m<sup>2</sup>) to study the effect of  $R$  on fatigue-crack growth. The test results were analyzed using the stress-intensity method and correlated with three empirical relations. The following conclusions can be drawn from this study:

1. In plots of crack-growth rates against the stress-intensity range, all of the data from tests at negative  $R$  values fell into a relatively narrow scatterband with the data from the  $R = 0$  tests indicating that the compression portion of the loading cycle did not significantly affect crack growth in these tests.
2. In contrast the data from all tests at a given positive  $R$  value fell into discrete bands in the plots of rate against stress-intensity range. These bands varied systematically with  $R$ , that is, the higher the stress ratio, the higher the rate of fatigue-crack growth for a given value of  $\Delta K$ . The spreads in rates for different values of  $R$  became larger as  $\Delta K$  increased.
3. Empirical equations developed by Forman, et al., and by Broek and Schijve which present the rate as a function of stress-intensity range, stress

ratio, and the critical stress-intensity factor for failure (Forman's equation only) were fitted to the data. Forman's equation produced an excellent fit to the data whereas Broek's equation did not correlate well at the higher crack-growth rates. Forman's equation can be used to predict fatigue-crack-growth behavior in 7075-T6 aluminum-alloy sheet for any loading condition for which the applied stress-intensity range can be calculated.

4. An empirical equation developed by Paris relating rate to the stress-intensity range produced a reasonably good fit to the data for a given value of  $R$ . However,  $R$  is not an explicit function in Paris' equation and individual constants are required for each value of  $R$ .

5. The fracture surfaces of the specimens changed from the normal mode to a shear mode within a reasonably narrow range of crack-growth rates for all  $R$  values.

6. The stress-intensity factor range at transition from the normal to the shear fracture mode was approximately a constant for tests at negative-stress ratios. Forman's equation adequately represented the variation between the stress ratio and the stress-intensity range at positive-stress ratios for transition conditions.

## APPENDIX

### CONVERSION OF U.S. CUSTOMARY UNITS TO SI UNITS

The International System of Units (SI) was adopted by the Eleventh General Conference of Weights and Measures, Paris, October 1960, in Resolution No. 12 (ref. 4). Conversion factors for the units used herein are given in the following table:

| To convert from<br>U.S. Customary Units | Multiply by           | To obtain SI Units                            |
|-----------------------------------------|-----------------------|-----------------------------------------------|
| lbf                                     | 4.448222              | newton (N)                                    |
| in.                                     | $2.54 \times 10^{-2}$ | meter (M)                                     |
| ksi                                     | 6.894757              | newton/meter <sup>2</sup> (N/m <sup>2</sup> ) |
| cpm                                     | $1.67 \times 10^{-2}$ | hertz (Hz)                                    |

Prefixes and symbols to indicate multiples of units are as follows:

| Multiple  | Prefix | Symbol |
|-----------|--------|--------|
| $10^{-9}$ | nano   | n      |
| $10^{-3}$ | milli  | m      |
| $10^3$    | kilo   | k      |
| $10^6$    | mega   | M      |
| $10^9$    | giga   | G      |

## REFERENCES

1. Paris, Paul C.: The Fracture Mechanics Approach to Fatigue. Fatigue - An Interdisciplinary Approach. John J. Burke, Norman L. Reed, and Volker Weiss, Syracuse Univ. Press, 1964.
2. Figge, I. E.; and Newman, J. C., Jr.: Fatigue Crack Propagation in Structures With Simulated Rivet Forces. Paper No. 30 presented at the ASTM Annual Meeting held in Atlantic City, June 27-July 1, 1966.
3. Forman, R. G.; Kearney, V. E.; and Engle, R. M.: Numerical Analysis of Crack Propagation in Cyclically Loaded Structures. Presented at the 1966 ASME Annual Winter Meeting. Paper No. 66, WA/MET-4, Nov. 1966.
4. Broek, D.; and Schijve, J.: The Influence of the Mean Stress on the Propagation of Fatigue Cracks in Aluminum Alloy Sheet. NLR-TR M.2111, 1963.
5. Mechtly, E. A.: The International System of Units - Physical Constants and Conversion Factors. NASA SP-7012, 1964.
6. Grover, H. J.; Bishop, S. M.; and Jackson, L. R.: Fatigue Strengths of Aircraft Materials. Axial-Load Fatigue Tests on Unnotched Sheet Specimens of 24S-T3 and 75S-T6 Aluminum Alloys and of SAE 4130 Steel. NACA TN 2324, 1951.
7. Hudson, C. Michael: Fatigue-Crack Propagation in Several Titanium and Stainless-Steel Alloys and One Superalloy. NASA TN D-2331, 1964.
8. Grover, H. J.; Hyler, W. S.; Kuhn, Paul; Landers, Charles B.; and Howell, F. M.: Axial-Load Fatigue Properties of 24S-T and 75S-T Aluminum Alloy as Determined at Several Laboratories. NACA Rept. 1190, 1954 (Supersedes NACA TN 2928).
9. McEvily, Arthur J., Jr.; and Illg, Walter: The Rate of Fatigue-Crack Propagation in Two Aluminum Alloys. NACA TN 4394, 1958.
10. Illg, Walter: Fatigue Tests on Notched and Unnotched Sheet Specimens Made of 2024-T3 and 7075-T6 Aluminum Alloys and of SAE 4130 Steel With Special Consideration of the Life Range From 2 to 10,000 Cycles. NACA TN 3866, 1956.
11. Hudson, C. Michael; and Hardrath, Herbert F.: Investigation of the Effects of Variable-Amplitude Loadings on Fatigue Crack Propagation Patterns. NASA TN D-1803, 1963.
12. Illg, Walter; and McEvily, Arthur J., Jr.: The Rate of Fatigue-Crack Propagation for Two Aluminum Alloys Under Completely Reversed Loading. NASA TN D-52, 1959.

13. Hudson, C. Michael: Investigation of Fatigue Crack Growth in Ti-8Al-1Mo-1V (Duplex Annealed) Specimens Having Various Widths. NASA TN D-3879, 1967.
14. Wilhem, D. P.: Crack Propagation and Stress Intensity Interrelationships Accompanying Fatigue on Sheet Materials. SESA Paper No. 1173, Nov. 1966.

TABLE I. - AVERAGE TENSILE PROPERTIES OF

THE 7075-T6 ALUMINUM-ALLOY TESTED

| Ultimate tensile strength |                   | Yield strength (0.2-percent offset) |                   | Young's modulus of elasticity |                   | Elongation in 2-inch (51 mm) gage length, percent | Number of tests |
|---------------------------|-------------------|-------------------------------------|-------------------|-------------------------------|-------------------|---------------------------------------------------|-----------------|
| ksi                       | MN/m <sup>2</sup> | ksi                                 | MN/m <sup>2</sup> | ksi                           | GN/m <sup>2</sup> |                                                   |                 |
| 82.9                      | 572               | 75.5                                | 521               | $10.2 \times 10^3$            | 70.3              | 12                                                | 152             |



TABLE II. - AVERAGE NUMBER OF CYCLES REQUIRED TO EXTEND CRACKS FROM A HALF-LENGTH OF 0.10 INCH (2.54 mm) IN 7075-T6 ALUMINUM-ALLOY SHEET

| S <sub>m</sub><br>ksi<br>MM/m <sup>2</sup> | S <sub>a</sub><br>ksi<br>MM/m <sup>2</sup> | Nominal<br>R value | Number of cycles required to propagate a crack from a half-length a of 0.10 in. (2.54 mm) to a half-length a of - |                       |                        |                        |                        |                        |                        |                        |                        |                        |                        |                        |                        |                        |
|--------------------------------------------|--------------------------------------------|--------------------|-------------------------------------------------------------------------------------------------------------------|-----------------------|------------------------|------------------------|------------------------|------------------------|------------------------|------------------------|------------------------|------------------------|------------------------|------------------------|------------------------|------------------------|
|                                            |                                            |                    | 0.20 in.<br>(5.08 mm)                                                                                             | 0.30 in.<br>(7.62 mm) | 0.40 in.<br>(10.16 mm) | 0.50 in.<br>(12.70 mm) | 0.60 in.<br>(15.24 mm) | 0.70 in.<br>(17.78 mm) | 0.80 in.<br>(20.32 mm) | 0.90 in.<br>(22.86 mm) | 1.00 in.<br>(25.40 mm) | 1.20 in.<br>(30.48 mm) | 1.40 in.<br>(35.56 mm) | 1.60 in.<br>(40.64 mm) | 1.80 in.<br>(45.72 mm) | 2.00 in.<br>(50.80 mm) |
| 0                                          | 0                                          | 0                  | 1,240                                                                                                             | 1,640                 | 1,865                  | 1,980                  | 2,040                  | 2,080                  | 2,110                  | 2,120                  | 2,140                  | 2,150                  | 2,160                  | 2,170                  | 2,180                  | 2,190                  |
| 0                                          | 0                                          | 0                  | 3,230                                                                                                             | 4,200                 | 4,860                  | 5,100                  | 5,160                  | 5,170                  | 5,180                  | 5,190                  | 5,200                  | 5,210                  | 5,220                  | 5,230                  | 5,240                  | 5,250                  |
| 0                                          | 0                                          | 0                  | 8,820                                                                                                             | 7,170                 | 8,450                  | 9,180                  | 9,600                  | 9,900                  | 10,060                 | 10,200                 | 10,300                 | 10,400                 | 10,500                 | 10,600                 | 10,700                 | 10,800                 |
| 0                                          | 0                                          | 0                  | 8,000                                                                                                             | 12,500                | 15,300                 | 17,300                 | 18,830                 | 19,900                 | 20,700                 | 21,300                 | 21,800                 | 22,300                 | 22,800                 | 23,300                 | 23,800                 | 24,300                 |
| 0                                          | 0                                          | 0                  | 30,000                                                                                                            | 45,800                | 52,000                 | 58,100                 | 63,400                 | 67,500                 | 71,000                 | 74,000                 | 76,800                 | 79,500                 | 82,000                 | 84,500                 | 87,000                 | 89,500                 |
| 0                                          | 0                                          | 0                  | 492,000                                                                                                           | 770,000               | 867,000                | 960,000                | 960,000                | 985,000                | 1,007,000              | 1,020,000              | 1,040,000              | 1,065,000              | 1,085,000              | 1,110,000              | 1,135,000              | 1,158,000              |
| 2.5                                        | 17                                         | 20                 | 2,500                                                                                                             | 3,730                 | 4,380                  | 4,760                  | 5,000                  | 5,150                  | 5,280                  | 5,370                  | 5,440                  | 5,500                  | 5,560                  | 5,620                  | 5,680                  | 5,740                  |
| 2.5                                        | 17                                         | 17.5               | 5,720                                                                                                             | 8,700                 | 10,080                 | 10,860                 | 11,370                 | 11,700                 | 11,980                 | 12,120                 | 12,260                 | 12,400                 | 12,540                 | 12,680                 | 12,820                 | 12,960                 |
| 5                                          | 34                                         | 25                 | 1,375                                                                                                             | 1,900                 | 2,160                  | 2,320                  | 2,410                  | 2,475                  | 2,525                  | 2,570                  | 2,600                  | 2,640                  | 2,680                  | 2,720                  | 2,760                  | 2,800                  |
| 2.5                                        | 17                                         | 10.5               | 5,900                                                                                                             | 8,300                 | 10,200                 | 11,300                 | 12,130                 | 12,700                 | 13,200                 | 13,570                 | 13,780                 | 14,100                 | 14,360                 | 14,600                 | 14,800                 | 15,000                 |
| 2.5                                        | 17                                         | 12.5               | 11,400                                                                                                            | 16,800                | 20,100                 | 22,200                 | 23,800                 | 24,800                 | 25,600                 | 26,200                 | 26,700                 | 27,100                 | 27,400                 | 27,700                 | 28,000                 | 28,300                 |
| 5                                          | 34                                         | 20                 | 2,640                                                                                                             | 3,740                 | 4,300                  | 4,640                  | 4,850                  | 5,000                  | 5,100                  | 5,170                  | 5,230                  | 5,270                  | 5,310                  | 5,350                  | 5,390                  | 5,430                  |
| 2.5                                        | 17                                         | 10                 | 16,600                                                                                                            | 24,200                | 28,500                 | 31,700                 | 34,000                 | 35,800                 | 37,400                 | 38,700                 | 39,900                 | 41,100                 | 42,300                 | 43,500                 | 44,700                 | 45,900                 |
| 5                                          | 34                                         | 15                 | 5,300                                                                                                             | 7,900                 | 9,730                  | 10,680                 | 11,200                 | 11,550                 | 11,800                 | 11,970                 | 12,060                 | 12,200                 | 12,340                 | 12,480                 | 12,620                 | 12,760                 |
| 10                                         | 69                                         | 20                 | 1,550                                                                                                             | 2,100                 | 2,350                  | 2,470                  | 2,540                  | 2,580                  | 2,600                  | 2,630                  | 2,653                  | 2,677                  | 2,701                  | 2,725                  | 2,749                  | 2,773                  |
| 5                                          | 34                                         | 10                 | 12,300                                                                                                            | 18,300                | 22,000                 | 24,500                 | 26,600                 | 28,200                 | 29,300                 | 30,200                 | 30,900                 | 31,600                 | 32,300                 | 33,000                 | 33,700                 | 34,400                 |
| 2.5                                        | 17                                         | 5                  | 140,000                                                                                                           | 186,000               | 209,000                | 223,000                | 233,000                | 241,000                | 246,000                | 252,000                | 257,000                | 264,000                | 270,000                | 276,000                | 282,000                | 288,000                |
| 20                                         | 138                                        | 30                 | 226                                                                                                               | 294                   | 316                    | 322                    | 324                    | 324                    | 324                    | 324                    | 324                    | 324                    | 324                    | 324                    | 324                    | 324                    |
| 10                                         | 69                                         | 15                 | 2,900                                                                                                             | 4,300                 | 4,930                  | 5,300                  | 5,540                  | 5,700                  | 5,800                  | 5,900                  | 5,990                  | 6,100                  | 6,160                  | 6,220                  | 6,280                  | 6,340                  |
| 15                                         | 103                                        | 20                 | 1,060                                                                                                             | 1,380                 | 1,545                  | 1,630                  | 1,680                  | 1,710                  | 1,730                  | 1,750                  | 1,770                  | 1,790                  | 1,810                  | 1,830                  | 1,850                  | 1,870                  |
| 25                                         | 172                                        | 25                 | 330                                                                                                               | 415                   | 475                    | 500                    | 515                    | 525                    | 535                    | 545                    | 555                    | 565                    | 575                    | 585                    | 595                    | 605                    |
| 20                                         | 138                                        | 20                 | 700                                                                                                               | 930                   | 1,030                  | 1,075                  | 1,100                  | 1,110                  | 1,115                  | 1,120                  | 1,125                  | 1,130                  | 1,135                  | 1,140                  | 1,145                  | 1,150                  |
| 15                                         | 103                                        | 15                 | 1,670                                                                                                             | 2,360                 | 2,660                  | 2,820                  | 2,930                  | 3,000                  | 3,050                  | 3,090                  | 3,130                  | 3,170                  | 3,210                  | 3,250                  | 3,290                  | 3,330                  |
| 10                                         | 69                                         | 10                 | 6,140                                                                                                             | 8,800                 | 10,370                 | 11,300                 | 11,800                 | 12,300                 | 12,570                 | 12,800                 | 12,950                 | 13,100                 | 13,250                 | 13,400                 | 13,550                 | 13,700                 |
| 5                                          | 34                                         | 5                  | 70,000                                                                                                            | 88,300                | 98,300                 | 105,000                | 110,000                | 113,000                | 115,000                | 117,000                | 119,000                | 121,000                | 123,000                | 125,000                | 127,000                | 129,000                |
| 30                                         | 207                                        | 20                 | 410                                                                                                               | 490                   | 560                    | 590                    | 610                    | 630                    | 650                    | 670                    | 690                    | 710                    | 730                    | 750                    | 770                    | 790                    |
| 25                                         | 172                                        | 16.7               | 760                                                                                                               | 990                   | 1,100                  | 1,150                  | 1,180                  | 1,200                  | 1,220                  | 1,240                  | 1,260                  | 1,280                  | 1,300                  | 1,320                  | 1,340                  | 1,360                  |
| 20                                         | 138                                        | 13.3               | 1,680                                                                                                             | 2,340                 | 2,640                  | 2,850                  | 2,960                  | 3,060                  | 3,120                  | 3,180                  | 3,240                  | 3,300                  | 3,360                  | 3,420                  | 3,480                  | 3,540                  |
| 15                                         | 103                                        | 10                 | 3,800                                                                                                             | 5,650                 | 6,550                  | 7,150                  | 7,500                  | 7,750                  | 7,950                  | 8,080                  | 8,190                  | 8,300                  | 8,420                  | 8,540                  | 8,660                  | 8,780                  |
| 30                                         | 207                                        | 15                 | 810                                                                                                               | 1,050                 | 1,130                  | 1,170                  | 1,200                  | 1,230                  | 1,260                  | 1,290                  | 1,320                  | 1,350                  | 1,380                  | 1,410                  | 1,440                  | 1,470                  |
| 25                                         | 172                                        | 12.5               | 1,500                                                                                                             | 2,060                 | 2,320                  | 2,470                  | 2,570                  | 2,650                  | 2,680                  | 2,710                  | 2,740                  | 2,770                  | 2,800                  | 2,830                  | 2,860                  | 2,890                  |
| 20                                         | 138                                        | 10                 | 3,040                                                                                                             | 4,260                 | 4,900                  | 5,280                  | 5,550                  | 5,720                  | 5,850                  | 5,940                  | 6,030                  | 6,120                  | 6,210                  | 6,300                  | 6,390                  | 6,480                  |
| 15                                         | 103                                        | 7.5                | 7,350                                                                                                             | 10,100                | 11,700                 | 12,800                 | 13,500                 | 14,000                 | 14,400                 | 14,800                 | 15,200                 | 15,600                 | 16,000                 | 16,400                 | 16,800                 | 17,200                 |
| 10                                         | 69                                         | 5                  | 16,100                                                                                                            | 23,700                | 28,300                 | 32,600                 | 35,500                 | 37,800                 | 39,500                 | 40,800                 | 42,000                 | 43,500                 | 44,800                 | 46,100                 | 47,400                 | 48,700                 |
| 30                                         | 207                                        | 10                 | 2,230                                                                                                             | 3,040                 | 3,430                  | 3,660                  | 3,810                  | 3,920                  | 3,990                  | 4,060                  | 4,130                  | 4,200                  | 4,270                  | 4,340                  | 4,410                  | 4,480                  |
| 25                                         | 172                                        | 8.3                | 4,100                                                                                                             | 5,600                 | 6,380                  | 6,800                  | 7,100                  | 7,260                  | 7,380                  | 7,480                  | 7,580                  | 7,680                  | 7,780                  | 7,880                  | 7,980                  | 8,080                  |
| 20                                         | 138                                        | 6.7                | 9,500                                                                                                             | 12,400                | 13,820                 | 14,730                 | 15,400                 | 15,900                 | 16,300                 | 16,700                 | 17,100                 | 17,500                 | 17,900                 | 18,300                 | 18,700                 | 19,100                 |
| 15                                         | 103                                        | 5                  | 18,500                                                                                                            | 28,000                | 32,800                 | 35,600                 | 37,600                 | 39,000                 | 40,000                 | 40,800                 | 41,400                 | 42,000                 | 42,500                 | 43,000                 | 43,500                 | 44,000                 |
| 10                                         | 69                                         | 3                  | 105,000                                                                                                           | 140,000               | 160,000                | 175,000                | 185,000                | 192,500                | 197,500                | 202,500                | 205,000                | 212,000                | 215,000                | 217,500                | 220,000                | 222,500                |
| 30                                         | 207                                        | 5                  | 12,300                                                                                                            | 16,300                | 18,300                 | 19,400                 | 20,200                 | 20,700                 | 21,000                 | 21,300                 | 21,600                 | 21,900                 | 22,200                 | 22,500                 | 22,800                 | 23,100                 |
| 25                                         | 172                                        | 4.4                | 19,800                                                                                                            | 27,000                | 30,900                 | 33,500                 | 35,200                 | 36,000                 | 36,500                 | 37,000                 | 37,500                 | 38,000                 | 38,500                 | 39,000                 | 39,500                 | 40,000                 |
| 20                                         | 138                                        | 3                  | 69,000                                                                                                            | 97,000                | 112,000                | 121,000                | 127,000                | 130,000                | 134,000                | 136,000                | 138,000                | 141,000                | 143,000                | 145,000                | 147,000                | 149,000                |
| 15                                         | 103                                        | 3                  | 115,000                                                                                                           | 155,000               | 185,000                | 205,000                | 225,000                | 245,000                | 265,000                | 285,000                | 305,000                | 325,000                | 345,000                | 365,000                | 385,000                | 405,000                |
| 10                                         | 69                                         | 1.7                | 780,000                                                                                                           | 1,260,000             | 1,540,000              | 1,690,000              | 1,780,000              | 1,825,000              | 1,850,000              | 1,870,000              | 1,885,000              | 1,915,000              | 1,930,000              | 1,945,000              | 1,960,000              | 1,975,000              |
| 30                                         | 207                                        | 3                  | 42,500                                                                                                            | 58,750                | 68,750                 | 75,000                 | 77,500                 | 80,000                 | 82,000                 | 83,750                 | 84,000                 | 85,000                 | 86,000                 | 87,000                 | 88,000                 | 89,000                 |
| 25                                         | 172                                        | 2.8                | 71,000                                                                                                            | 94,000                | 106,000                | 111,000                | 116,000                | 120,000                | 122,000                | 123,000                | 124,000                | 125,000                | 126,000                | 127,000                | 128,000                | 129,000                |

TABLE III.- CRACK AND LOAD MEASUREMENTS AND  $K_c$  VALUES  
 FROM RESIDUAL STATIC STRENGTH TESTS ON  
 7075-T6 ALUMINUM-ALLOY SHEET

| $a_i$ |       | $a_f$ |       | $P_i$ |     | $P_f$ |     | $K_c$                 |                     |
|-------|-------|-------|-------|-------|-----|-------|-----|-----------------------|---------------------|
| in.   | mm    | in.   | mm    | kips  | kN  | kips  | kN  | ksi-in <sup>1/2</sup> | MN/m <sup>3/2</sup> |
| 1.72  | 43.67 | 1.85  | 46.99 | 23.4  | 104 | 29.9  | 133 | 39.2                  | 43.1                |
| 1.59  | 40.39 | 1.80  | 45.72 | 17.7  | 79  | 30.4  | 135 | 39.2                  | 43.1                |
| 1.53  | 38.86 | 1.79  | 45.34 | 20.0  | 89  | 30.4  | 135 | 38.5                  | 42.3                |
| 1.94  | 49.15 | 2.36  | 59.95 | 16.5  | 73  | 27.2  | 121 | 39.8                  | 43.7                |
| 1.02  | 25.91 | 1.16  | 29.47 | ----  | --- | 38.5  | 171 | 38.0                  | 41.7                |
| .98   | 24.89 | 1.19  | 30.10 | ----  | --- | 38.8  | 173 | 39.7                  | 43.7                |
| .91   | 22.99 | .96   | 24.39 | ----  | --- | 43.1  | 192 | 38.0                  | 41.7                |
| 1.01  | 25.65 | 1.09  | 27.56 | ----  | --- | 41.7  | 185 | 41.4                  | 45.5                |
| 1.05  | 26.67 | 1.15  | 29.21 | 29.2  | 130 | 37.7  | 168 | 38.4                  | 42.2                |
| .78   | 19.81 | .94   | 23.75 | 32.8  | 146 | 44.5  | 198 | 41.6                  | 45.7                |
| 1.31  | 33.27 | 1.75  | 44.45 | 19.2  | 85  | 32.0  | 142 | 40.2                  | 44.2                |
| 1.90  | 48.26 | 2.19  | 55.63 | 15.7  | 70  | 25.0  | 111 | 35.4                  | 39.0                |
| .52   | 13.21 | .73   | 18.42 | 32.8  | 146 | 50.4  | 224 | 40.4                  | 44.4                |
| 1.22  | 30.99 | 1.53  | 38.86 | 25.8  | 115 | 35.9  | 160 | 42.0                  | 46.2                |
| 1.76  | 44.71 | 2.10  | 53.34 | 18.3  | 81  | 30.2  | 134 | 41.8                  | 45.9                |
| 1.40  | 35.44 | 1.73  | 43.82 | 26.8  | 119 | 32.3  | 144 | 41.0                  | 45.1                |
| 1.17  | 29.59 | 1.43  | 36.20 | 29.2  | 130 | 36.4  | 162 | 40.2                  | 44.2                |
| .54   | 13.72 | .71   | 17.91 | 33.3  | 148 | 49.8  | 222 | 38.5                  | 42.3                |
| 1.51  | 38.23 | 1.65  | 41.91 | 24.0  | 107 | 39.0  | 173 | 47.6                  | 52.3                |
| 2.25  | 57.15 | 2.73  | 69.34 | 12.3  | 54  | 24.3  | 108 | 41.0                  | 45.0                |
| 2.47  | 62.87 | 2.81  | 71.38 | 14.0  | 62  | 22.8  | 101 | 39.0                  | 42.9                |
| 1.78  | 45.09 | 2.13  | 53.98 | 14.8  | 66  | 27.1  | 121 | 39.0                  | 42.9                |
| .70   | 17.78 | .93   | 23.50 | ----  | --- | 47.1  | 210 | 43.4                  | 47.7                |
| .53   | 13.46 | .78   | 19.69 | 29.4  | 131 | 48.4  | 215 | 40.3                  | 44.3                |
| 1.07  | 27.18 | 1.20  | 30.48 | 30.0  | 133 | 39.0  | 173 | 48.2                  | 52.9                |
| 1.12  | 28.32 | 1.37  | 34.80 | 30.0  | 133 | 36.0  | 160 | 39.4                  | 43.3                |
| .55   | 13.97 | .72   | 18.29 | ----  | --- | 47.5  | 211 | 37.6                  | 41.3                |

TABLE IV.- TRANSITION CRACK LENGTHS AND CRACK-GROWTH RATES FOR R VALUES  
FROM -1.0 TO 0.8 FOR 7075-T6 ALUMINUM-ALLOY SHEET

| $S_m^i$ |                   | $S_a^i$ |                   | Nominal<br>R value | $a_t$ |       | da/dN at transition     |          | $\Delta K_t$          |                     | Type of shear |
|---------|-------------------|---------|-------------------|--------------------|-------|-------|-------------------------|----------|-----------------------|---------------------|---------------|
| ksi     | MN/m <sup>2</sup> | ksi     | MN/m <sup>2</sup> |                    | in.   | mm    | in./cycle               | mm/cycle | ksi-in <sup>1/2</sup> | MN/m <sup>3/2</sup> |               |
| 0       | 0                 | 30      | 207               | -1                 | ≤.05  | ≤1.3  | -----                   | ---      | ---                   | ---                 | Dual          |
| 0       | 0                 | 30      | 207               | -1                 | ≤.05  | ≤1.3  | -----                   | ---      | ---                   | ---                 | Single        |
| 0       | 0                 | 25      | 172               | -1                 | ≤.05  | ≤1.3  | -----                   | ---      | ---                   | ---                 | Dual          |
| 0       | 0                 | 25      | 172               | -1                 | ≤.05  | ≤1.3  | -----                   | ---      | ---                   | ---                 | Single        |
| 0       | 0                 | 20      | 138               | -1                 | ≤.05  | ≤1.3  | -----                   | ---      | ---                   | ---                 | Dual          |
| 0       | 0                 | 20      | 138               | -1                 | ----- | ----- | -----                   | ---      | ---                   | ---                 | -----         |
| 0       | 0                 | 15      | 103               | -1                 | .13   | 3.3   | 1.08 × 10 <sup>-5</sup> | 274      | 5.4                   | 5.9                 | Dual          |
| 0       | 0                 | 15      | 103               | -1                 | .17   | 4.3   | 1.49 × 10 <sup>-5</sup> | 379      | 6.3                   | 6.9                 | Single        |
| 0       | 0                 | 10      | 69                | -1                 | .37   | 9.4   | 1.37 × 10 <sup>-5</sup> | 348      | 6.0                   | 6.6                 | Double        |
| 0       | 0                 | 10      | 69                | -1                 | ----- | ----- | -----                   | ---      | ---                   | ---                 | -----         |
| 0       | 0                 | 5       | 34                | -1                 | 1.16  | 58.9  | 9.67 × 10 <sup>-6</sup> | 246      | 5.4                   | 5.9                 | Double        |
| 0       | 0                 | 5       | 34                | -1                 | 1.64  | 41.7  | 1.64 × 10 <sup>-5</sup> | 417      | 6.5                   | 7.1                 | Dual          |
| 2.5     | 17                | 20      | 138               | -.8                | ≤.05  | ≤1.3  | -----                   | ---      | ---                   | ---                 | Dual          |
| 2.5     | 17                | 20      | 138               | -.8                | ≤.05  | ≤1.3  | -----                   | ---      | ---                   | ---                 | Single        |
| 2.5     | 17                | 17.5    | 121               | -.8                | ≤.05  | ≤1.3  | -----                   | ---      | ---                   | ---                 | Dual          |
| 2.5     | 17                | 17.5    | 121               | -.8                | .12   | 3.1   | 1.18 × 10 <sup>-5</sup> | 300      | 6.9                   | 7.6                 | Dual          |
| 5       | 34                | 25      | 172               | -.7                | ≤.05  | ≤1.3  | -----                   | ---      | ---                   | ---                 | Single        |
| 5       | 34                | 25      | 172               | -.7                | ≤.05  | ≤1.3  | -----                   | ---      | ---                   | ---                 | Double        |
| 2.5     | 17                | 15      | 103               | -.7                | .18   | 4.6   | 2.53 × 10 <sup>-5</sup> | 643      | 7.3                   | 8.0                 | Dual          |
| 2.5     | 17                | 15      | 103               | -.7                | .20   | 5.1   | 2.78 × 10 <sup>-5</sup> | 706      | 7.8                   | 8.6                 | Dual          |
| 2.5     | 17                | 12.5    | 86                | -.7                | .16   | 4.1   | 1.03 × 10 <sup>-5</sup> | 262      | 5.9                   | 6.5                 | Dual          |
| 2.5     | 17                | 12.5    | 86                | -.7                | .28   | 7.1   | 2.31 × 10 <sup>-5</sup> | 587      | 7.9                   | 8.7                 | Dual          |
| 5       | 34                | 20      | 138               | -.6                | ≤.05  | ≤1.3  | -----                   | ---      | ---                   | ---                 | Double        |
| 5       | 34                | 20      | 138               | -.6                | .10   | 2.5   | 2.31 × 10 <sup>-5</sup> | 587      | 7.9                   | 8.7                 | Dual          |
| 2.5     | 17                | 10      | 69                | -.6                | .22   | 5.6   | 1.24 × 10 <sup>-5</sup> | 315      | 5.8                   | 6.4                 | Dual          |
| 2.5     | 17                | 10      | 69                | -.6                | .31   | 7.9   | 2.09 × 10 <sup>-5</sup> | 531      | 6.9                   | 7.6                 | Double        |
| 5       | 34                | 15      | 103               | -.5                | ≤.05  | ≤1.3  | -----                   | ---      | ---                   | ---                 | Single        |
| 5       | 34                | 15      | 103               | -.5                | ≤.05  | ≤1.3  | -----                   | ---      | ---                   | ---                 | Single        |
| 10      | 69                | 20      | 138               | -.33               | ≤.05  | ≤1.3  | -----                   | ---      | ---                   | ---                 | Single        |
| 10      | 69                | 20      | 138               | -.33               | ≤.05  | ≤1.3  | -----                   | ---      | ---                   | ---                 | Dual          |
| 5       | 34                | 10      | 69                | -.33               | .17   | 4.2   | 9.48 × 10 <sup>-6</sup> | 241      | 6.1                   | 6.7                 | Single        |
| 5       | 34                | 10      | 69                | -.33               | .21   | 5.3   | 1.27 × 10 <sup>-5</sup> | 323      | 6.8                   | 7.5                 | Single        |
| 2.5     | 17                | 5       | 34                | -.33               | .67   | 17.0  | 1.49 × 10 <sup>-5</sup> | 379      | 6.0                   | 6.6                 | Double        |
| 2.5     | 17                | 5       | 34                | -.33               | .77   | 14.6  | 1.54 × 10 <sup>-5</sup> | 391      | 6.5                   | 7.1                 | Double        |
| 20      | 138               | 30      | 207               | -.2                | ≤.05  | ≤1.3  | -----                   | ---      | ---                   | ---                 | Dual          |
| 20      | 138               | 30      | 207               | -.2                | ≤.05  | ≤1.3  | -----                   | ---      | ---                   | ---                 | Dual          |
| 10      | 69                | 15      | 103               | -.2                | ≤.05  | ≤1.3  | -----                   | ---      | ---                   | ---                 | Single        |
| 10      | 69                | 15      | 103               | -.2                | ≤.05  | ≤1.3  | -----                   | ---      | ---                   | ---                 | Dual          |
| 15      | 103               | 20      | 138               | -.14               | ≤.05  | ≤1.3  | -----                   | ---      | ---                   | ---                 | Single        |
| 15      | 103               | 20      | 138               | -.14               | ≤.05  | ≤1.3  | -----                   | ---      | ---                   | ---                 | Dual          |

TABLE IV. - TRANSITION CRACK LENGTHS AND CRACK-GROWTH RATES FOR R VALUES  
FROM -1.0 TO 0.8 FOR 7075-T6 ALUMINUM-ALLOY SHEET - Concluded

| $S_m^i$ |                   | $S_a^i$ |                   | Nominal<br>R value | $a_t$ |       | da/dN at transition                    |          | $\Delta K_t$          |                     | Type of shear |
|---------|-------------------|---------|-------------------|--------------------|-------|-------|----------------------------------------|----------|-----------------------|---------------------|---------------|
| ksi     | MN/m <sup>2</sup> | ksi     | MN/m <sup>2</sup> |                    | in.   | mm    | in./cycle                              | mm/cycle | ksi-in <sup>1/2</sup> | MN/m <sup>3/2</sup> |               |
| 25      | 172               | 25      | 172               | 0                  | ≤0.05 | ≤1.3  | -----                                  | ---      | ---                   | ---                 | Dual          |
| 25      | 172               | 25      | 172               | 0                  | ≤0.05 | ≤1.3  | -----                                  | ---      | ---                   | ---                 | Double        |
| 20      | 138               | 20      | 138               | 0                  | ≤0.05 | ≤1.3  | -----                                  | ---      | ---                   | ---                 | Dual          |
| 20      | 138               | 20      | 138               | 0                  | ≤0.05 | ≤1.3  | -----                                  | ---      | ---                   | ---                 | Dual          |
| 15      | 103               | 15      | 103               | 0                  | ≤0.05 | ≤1.3  | -----                                  | ---      | ---                   | ---                 | Dual          |
| 15      | 103               | 15      | 103               | 0                  | ≤0.05 | ≤1.3  | -----                                  | ---      | ---                   | ---                 | Dual          |
| 10      | 69                | 10      | 69                | 0                  | .11   | 2.8   | $1.06 \times 10^{-5}$                  | 269      | 6.5                   | 7.1                 | Double        |
| 10      | 69                | 10      | 69                | 0                  | .13   | 3.3   | $1.44 \times 10^{-5}$                  | 379      | 7.1                   | 7.8                 | Single        |
| 5       | 34                | 5       | 34                | 0                  | .52   | 13.2  | $1.53 \times 10^{-5}$                  | 389      | 7.1                   | 7.8                 | Dual          |
| 5       | 34                | 5       | 34                | 0                  | .61   | 15.5  | $2.54 \times 10^{-5}$                  | 645      | 7.7                   | 8.5                 | Dual          |
| 30      | 207               | 20      | 138               | .2                 | ≤0.05 | ≤1.3  | -----                                  | ---      | ---                   | ---                 | Single        |
| 30      | 207               | 20      | 138               | .2                 | ≤0.05 | ≤1.3  | -----                                  | ---      | ---                   | ---                 | Single        |
| 25      | 172               | 16.7    | 115               | .2                 | ≤0.05 | ≤1.3  | -----                                  | ---      | ---                   | ---                 | Single        |
| 25      | 172               | 16.7    | 115               | .2                 | ≤0.05 | ≤1.3  | -----                                  | ---      | ---                   | ---                 | Double        |
| 20      | 138               | 13.3    | 92                | .2                 | ≤0.05 | ≤1.3  | -----                                  | ---      | ---                   | ---                 | Dual          |
| 20      | 138               | 13.3    | 92                | .2                 | ≤0.05 | ≤1.3  | -----                                  | ---      | ---                   | ---                 | Dual          |
| 15      | 103               | 10      | 69                | .2                 | .08   | 2.0   | Crack length too short to measure rate |          | ---                   | ---                 | Single        |
| 15      | 103               | 10      | 69                | .2                 | .11   | 2.8   | $1.96 \times 10^{-5}$                  | 498      | 6.5                   | 7.1                 | Single        |
| 30      | 207               | 15      | 103               | .33                | ≤0.05 | ≤1.3  | -----                                  | ---      | ---                   | ---                 | Single        |
| 30      | 207               | 15      | 103               | .33                | ≤0.05 | ≤1.3  | -----                                  | ---      | ---                   | ---                 | Double        |
| 25      | 172               | 12.5    | 86                | .33                | ≤0.05 | ≤1.3  | -----                                  | ---      | ---                   | ---                 | Dual          |
| 25      | 172               | 12.5    | 86                | .33                | ≤0.05 | ≤1.3  | -----                                  | ---      | ---                   | ---                 | Dual          |
| 20      | 138               | 10      | 69                | .33                | ≤0.05 | ≤1.3  | -----                                  | ---      | ---                   | ---                 | Dual          |
| 20      | 138               | 10      | 69                | .33                | .10   | 2.7   | $2.31 \times 10^{-5}$                  | 587      | 6.3                   | 6.9                 | Double        |
| 15      | 103               | 7.5     | 52                | .33                | .15   | 3.8   | $1.90 \times 10^{-5}$                  | 483      | 5.8                   | 6.4                 | Dual          |
| 15      | 103               | 7.5     | 52                | .33                | .15   | 3.8   | $1.33 \times 10^{-5}$                  | 338      | 5.8                   | 6.4                 | Double        |
| 10      | 69                | 5       | 34                | .33                | .31   | 7.9   | $1.72 \times 10^{-5}$                  | 437      | 5.6                   | 6.2                 | Single        |
| 10      | 69                | 5       | 34                | .33                | .32   | 8.1   | $1.88 \times 10^{-5}$                  | 478      | 5.7                   | 6.3                 | Double        |
| 30      | 207               | 10      | 69                | .5                 | ≤0.05 | ≤1.3  | -----                                  | ---      | ---                   | ---                 | Dual          |
| 30      | 207               | 10      | 69                | .5                 | ≤0.05 | ≤1.3  | -----                                  | ---      | ---                   | ---                 | Single        |
| 25      | 172               | 8.3     | 57                | .5                 | ≤0.05 | ≤1.3  | -----                                  | ---      | ---                   | ---                 | Dual          |
| 25      | 172               | 8.3     | 57                | .5                 | ≤0.05 | ≤1.3  | -----                                  | ---      | ---                   | ---                 | Double        |
| 20      | 138               | 6.7     | 46                | .5                 | .18   | 4.6   | $1.80 \times 10^{-5}$                  | 457      | 5.5                   | 6.0                 | Double        |
| 20      | 138               | 6.7     | 46                | .5                 | .21   | 5.3   | $2.10 \times 10^{-5}$                  | 533      | 6.1                   | 6.7                 | Double        |
| 15      | 103               | 5       | 34                | .5                 | .21   | 5.3   | $8.08 \times 10^{-6}$                  | 205      | 4.6                   | 5.1                 | Dual          |
| 15      | 103               | 5       | 34                | .5                 | .30   | 7.6   | $2.00 \times 10^{-5}$                  | 508      | 5.5                   | 6.0                 | Double        |
| 10      | 69                | 3       | 21                | .5                 | .56   | 14.2  | $1.14 \times 10^{-5}$                  | 290      | 4.5                   | 4.9                 | Dual          |
| 10      | 69                | 3       | 21                | .5                 | .84   | 21.2  | $1.86 \times 10^{-5}$                  | 472      | 5.5                   | 6.0                 | Single        |
| 30      | 207               | 5       | 34                | .7                 | .17   | 4.3   | $1.07 \times 10^{-5}$                  | 273      | 4.1                   | 4.5                 | Double        |
| 30      | 207               | 5       | 34                | .7                 | .25   | 6.4   | $2.54 \times 10^{-5}$                  | 622      | 5.0                   | 5.5                 | Single        |
| 25      | 172               | 4.4     | 30                | .7                 | ----- | ----- | -----                                  | ---      | ---                   | ---                 | -----         |
| 25      | 172               | 4.4     | 30                | .7                 | .27   | 6.9   | $1.69 \times 10^{-5}$                  | 429      | 4.5                   | 4.9                 | Double        |
| 20      | 138               | 3       | 21                | .7                 | .44   | 11.1  | $1.21 \times 10^{-5}$                  | 307      | 3.9                   | 4.3                 | Dual          |
| 20      | 138               | 3       | 21                | .7                 | .50   | 12.7  | $1.72 \times 10^{-5}$                  | 437      | 4.2                   | 4.6                 | Dual          |
| 15      | 103               | 3       | 21                | .7                 | ----- | ----- | -----                                  | ---      | ---                   | ---                 | -----         |
| 15      | 103               | 3       | 21                | .7                 | .57   | 14.5  | $1.58 \times 10^{-5}$                  | 401      | 4.6                   | 5.1                 | Dual          |
| 10      | 69                | 1.7     | 12                | .7                 | 1.44  | 36.6  | $2.88 \times 10^{-5}$                  | 731      | 4.1                   | 4.5                 | Double        |
| 10      | 69                | 1.7     | 12                | .7                 | 1.53  | 38.9  | $2.55 \times 10^{-5}$                  | 648      | 4.3                   | 4.7                 | Double        |
| 30      | 207               | 3       | 21                | .8                 | ----- | ----- | -----                                  | ---      | ---                   | ---                 | -----         |
| 30      | 207               | 3       | 21                | .8                 | .43   | 10.9  | $1.92 \times 10^{-5}$                  | 488      | 4.0                   | 4.4                 | Double        |
| 25      | 172               | 2.8     | 19                | .8                 | .42   | 10.7  | $1.35 \times 10^{-5}$                  | 343      | 3.6                   | 4.0                 | Double        |
| 25      | 172               | 2.8     | 19                | .8                 | .55   | 13.9  | $2.20 \times 10^{-5}$                  | 559      | 4.1                   | 4.5                 | Dual          |

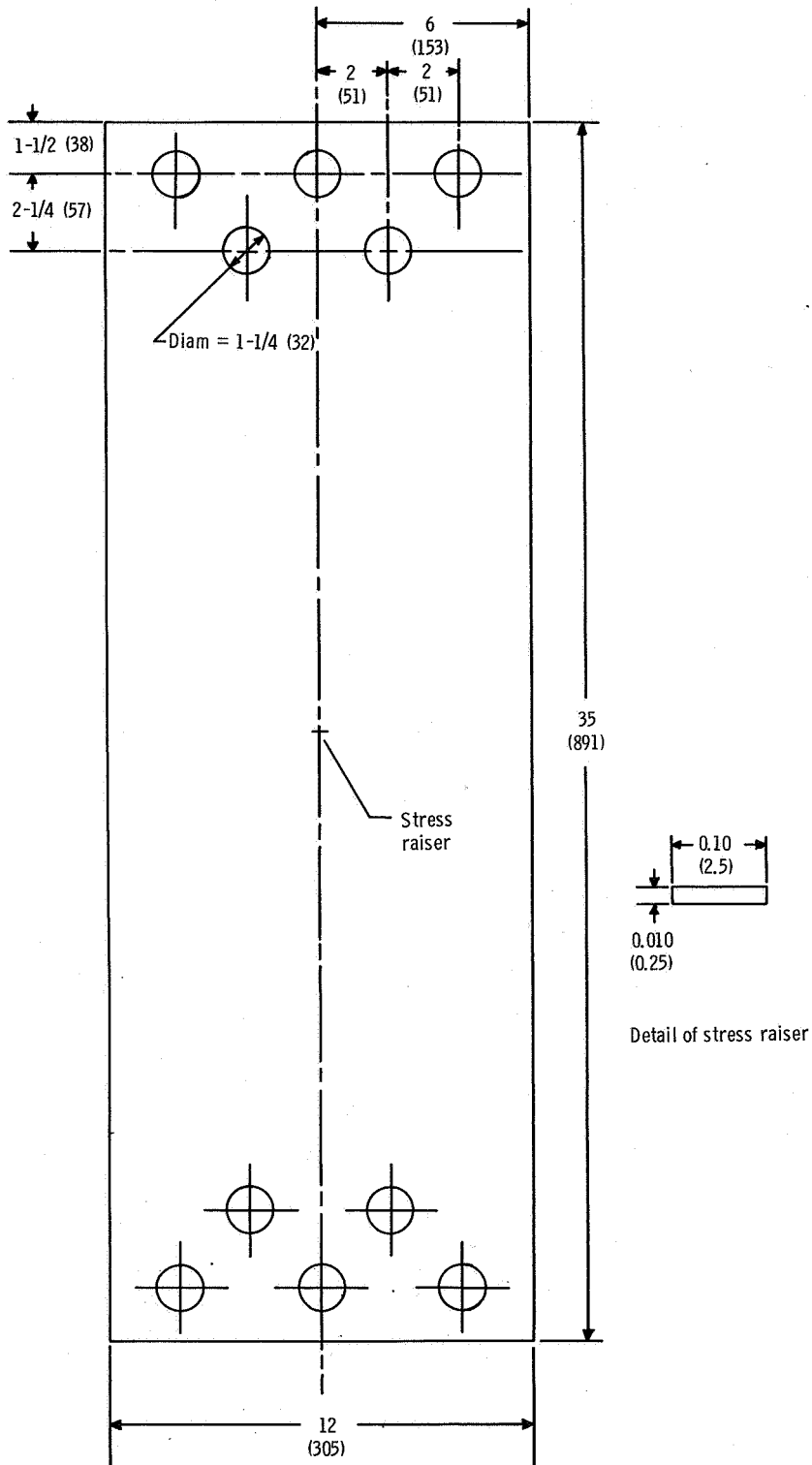


Figure 1.- Specimen configuration. All dimensions are in inches (mm).

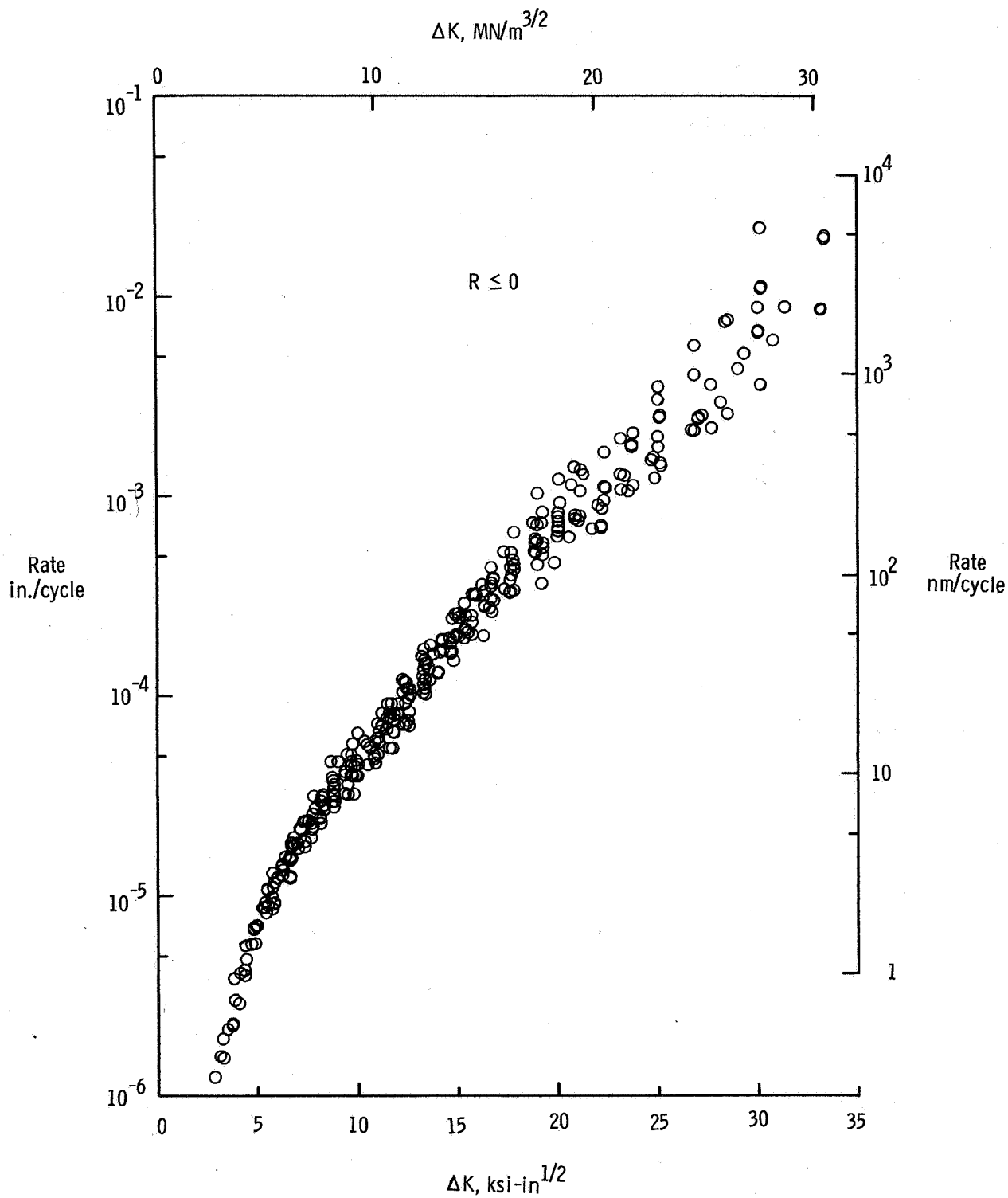


Figure 2.- Variation of fatigue crack growth rate with  $\Delta K$  for  $R \leq 0$ .

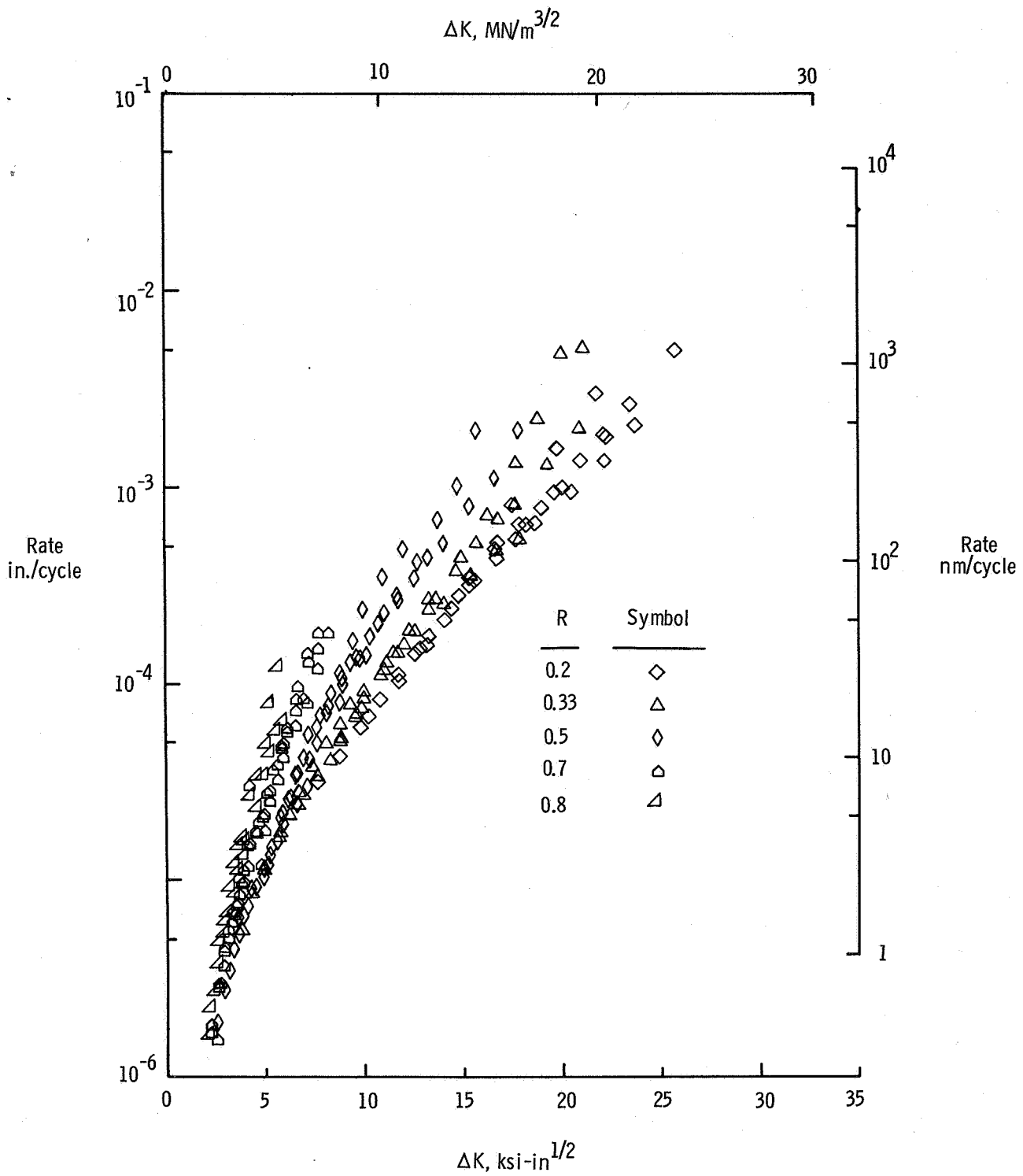


Figure 3.- Variation of fatigue crack growth rate with  $\Delta K$  for  $R > 0$ .

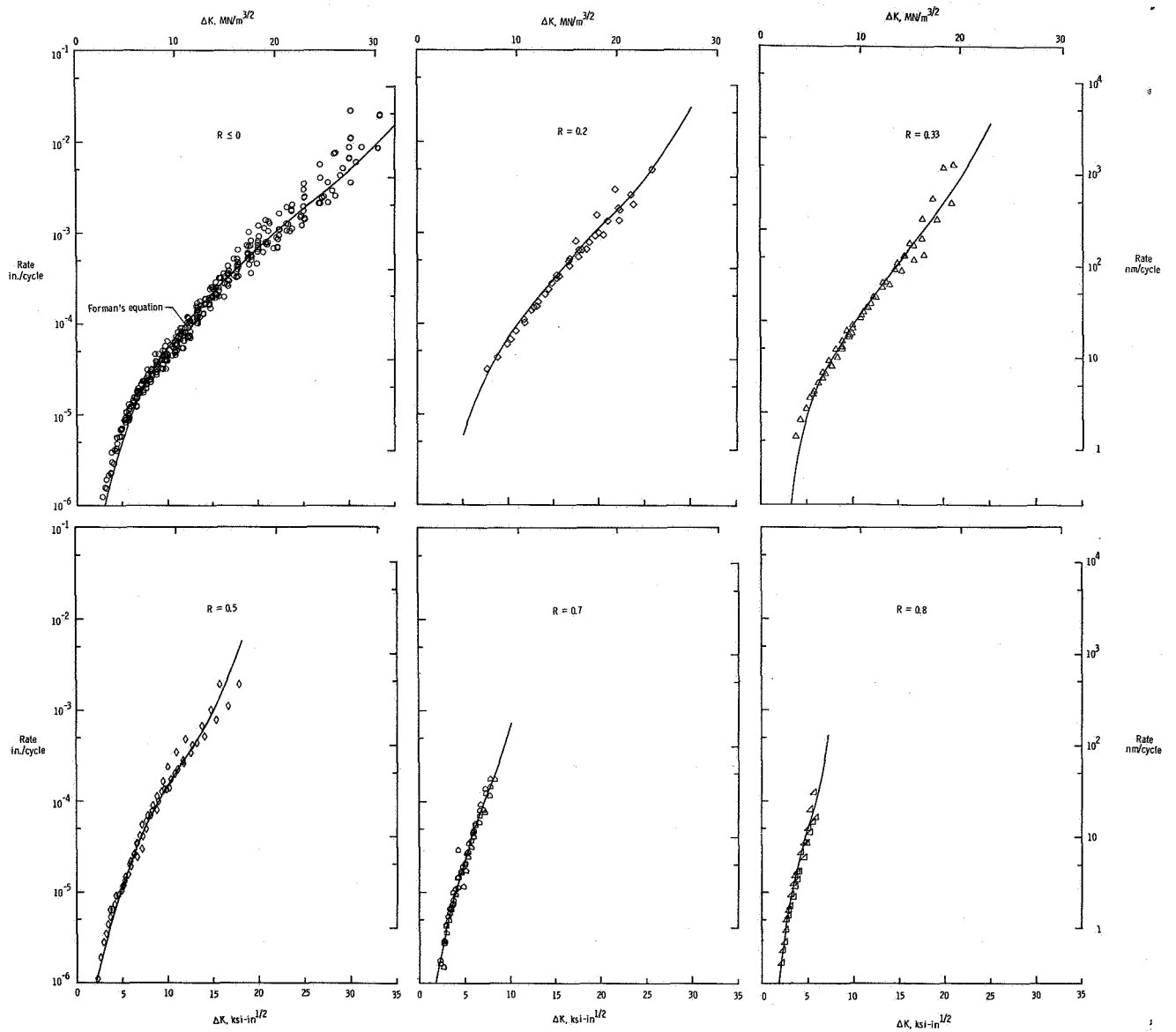


Figure 4.- Correlation of experimental fatigue crack growth rates at various stress ratios with Forman's equation.



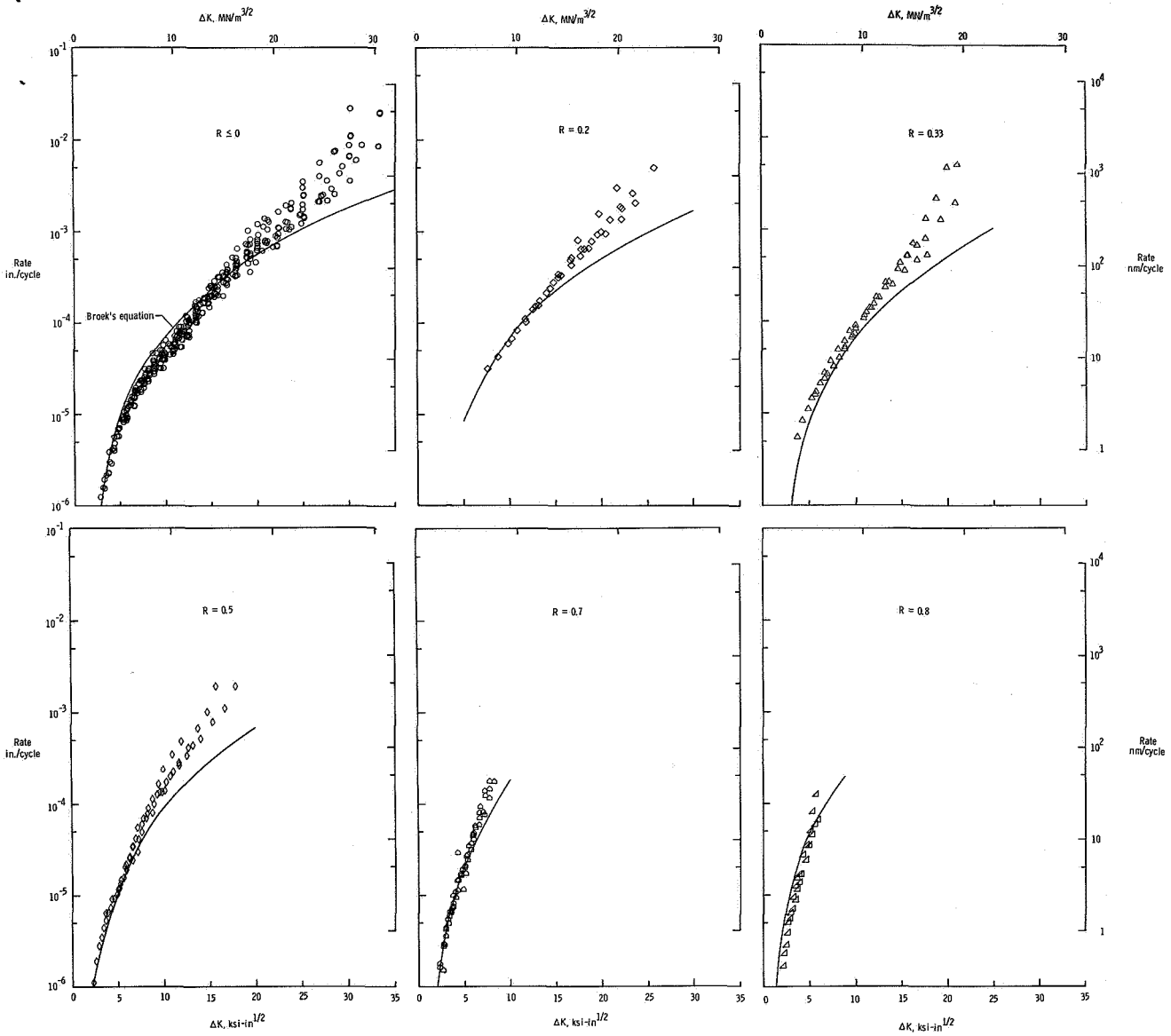


Figure 5.- Correlation of experimental fatigue crack growth rates at various stress ratios with Broek and Schijve's equation.

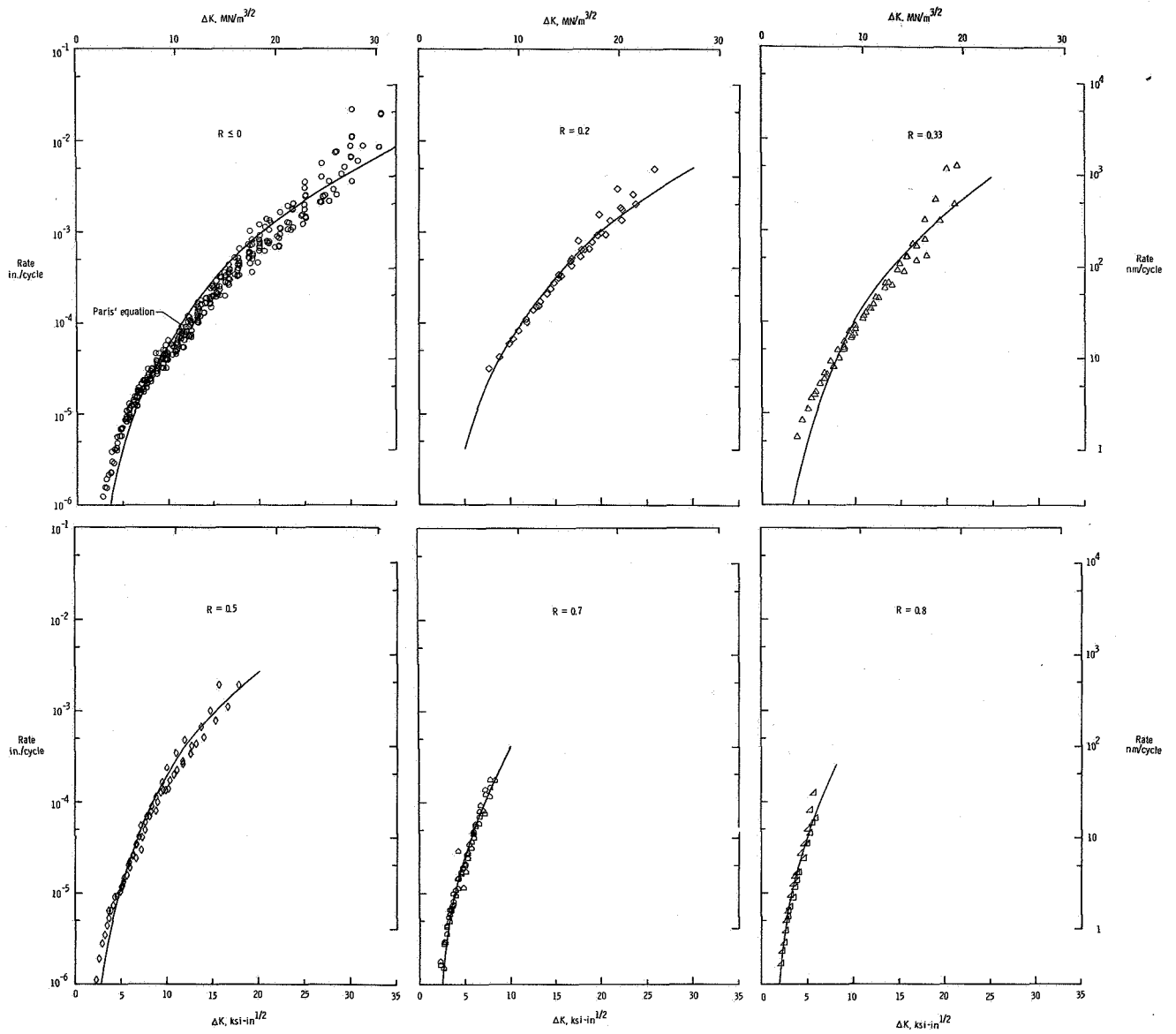


Figure 6.- Correlation of experimental fatigue crack growth rates at various stress ratios with Paris' equation.

$\Delta K$

$\text{MN}/\text{m}^{3/2}$        $\text{ksi}\cdot\text{in}^{1/2}$

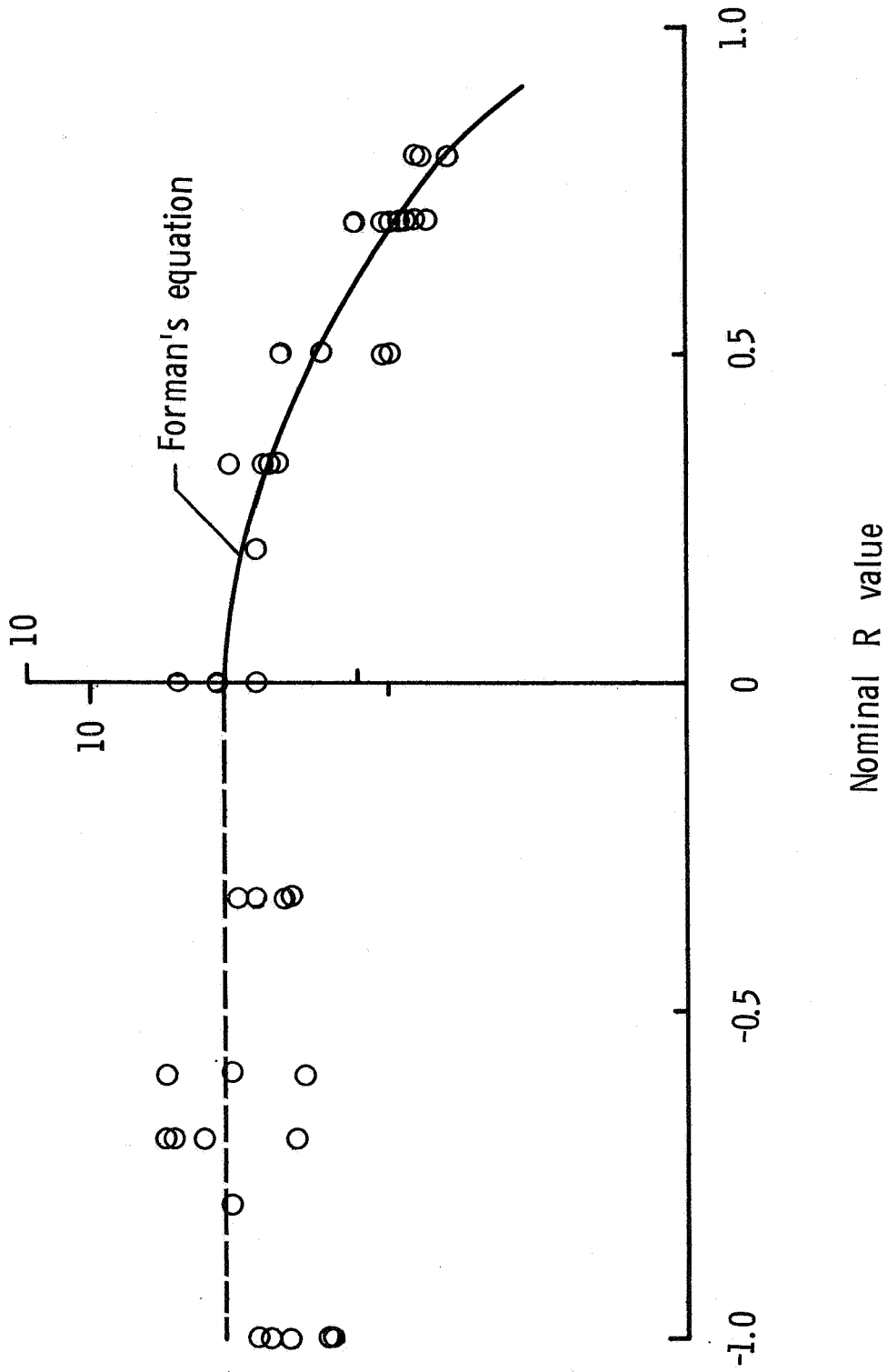


Figure 7.- Variation of the stress intensity range at transition from the normal mode to the shear mode with stress ratio.